Organic Electronics 14 (2013) 488–499

Contents lists available at SciVerse ScienceDirect

Organic Electronics

journal homepage: www.elsevier.com/locate/orgel

Single-component polyfluorene electrolytes bearing different counterions for white light-emitting electrochemical cells

Chia-Sheng Tsai, Sheng-Hsiung Yang *, Bo-Cun Liu, Hai-Ching Su *

Institute of Lighting and Energy Photonics, National Chiao Tung University, 301, Gaofa 3rd Road, Guiren Dist., Tainan 71150, Taiwan, ROC

ARTICLE INFO

Article history:
Received 22 October 2012
Received in revised form 15 November 2012
Accepted 28 November 2012
Available online 13 December 2012

Keywords:
Polyfluorene electrolytes
Counterions
Light-emitting electrochemical cells
Solid-state lighting

ABSTRACT

A series of polyfluorene (PF) electrolytes bearing Br^-, BF_4^-, or PF_6^- counterions were synthesized and characterized. 2,1,3-Benzoselenadiazole moieties were incorporated into polymer main chains to produce single-component white light-emitting polymers. The thermal stability of Br-containing ionic PF was decreased because of the Hofmann elimination occurred at higher temperature. By replacing Br^- with BF_4^- or PF_6^- counterions, the thermal stability of polymers was significantly improved. UV–vis absorption and photoluminescence spectra revealed that Br-containing ionic PF generates blue shift in methanol, while BF_4 and PF_6-containing ionic PFs show blue shift in acetonitrile. Electrochemical analysis revealed that oxidation potentials of BF_4 and PF_6-containing ionic PFs were decreased, resulting in increase in HOMO and LUMO levels. The optimized spin-coated light-emitting electrochemical cell (LEC) with the configuration of ITO/PEDOT/polymer/Ag showed a maximum luminescence efficiency of 1.56 lm/W at a low operation bias of 3 V. The single-component LEC device exhibited pure white light emission with CIE'1931 coordinates approaching (0.33, 0.33) and high color rendering index (CRI > 85), referring to its potential use in solid-state-lighting application.

1. Introduction

Organic polymers based on polyfluorene (PF) have widely been used in organic optoelectronic devices, such as organic light-emitting diodes (OLEDs), organic solar cells, and organic thin-film transistors [1–3]. PF and its derivatives, with their high photoluminescence (PL) quantum efficiencies, good thermal and chemical stability, excellent solubility in common organic solvents, are often used as good blue-light emitters. By properly adjusting the chemical structure and/or copolymerizing with suitable co-monomers, one can fine-tune their optical and electrical properties to obtain red, green, and even white emission [4–6]. Apart from being emitters in OLEDs, PF electrolytes carrying ionic groups on the end of C-9 substituents are also synthesized and utilized as electron-transporting layer to help carrier transport and to increase luminescence efficiency of devices [7–10].

Light-emitting electrochemical cells (LECs), demonstrated by Pei et al. in 1995, have drawn a great deal of attention in the area of organic light-emitting devices [11]. The device structure of LECs is constructed as sandwiched layer with the configuration of anode/emissive layer/cathode, using organic materials blended with inorganic salts as active layer. The function of added salts includes better carrier transport and lower operation voltage [12]. Two principal models, the electrochemical model [11,13], and the electrodynamic model [14,15], propose different working mechanisms of LECs. In the electrochemical model, the *p*-doped and *n*-doped regions are formed near the anode and cathode, respectively, under bias operation. The *p*–*i*–*n* interface is then constructed, confining emissive species in the intrinsic region [16]. The electrodynamic model depicts a strong decrease in

* Corresponding authors. Tel.: +886 6 3032121x57794; fax: +886 6 3032535 (S.H. Yang), tel.: +886 6 3032121x57792; fax: +886 6 3032535 (H.C. Su).

E-mail addresses: yangsh@mail.nctu.edu.tw (S.-H. Yang), haichingsu@mail.nctu.edu.tw (H.-C. Su).

1566-1199/$ - see front matter © 2012 Elsevier B.V. All rights reserved.
http://dx.doi.org/10.1016/j.orgel.2012.11.029

the injection barrier by the accumulation of ions at the interface. The electrochemical model predicts that most electric field drops across the intrinsic layer between the *p*- and *n*-doped layers while most electric field drops over a thin electrical double layer at the electrode interfaces in the electrodynamic model. Recently, several works showing evidence for either one or both of these models were presented [17–20]. Therefore, working mechanisms of LECs are still in debate up to now. The phase separation between organic materials and ionic salts are usually observed, resulting in reduced device performance for traditional LECs.

Considering the advantages of low voltage operation and simple layered structure, LECs are especially suitable for the application in solid-state lighting that requires high luminous efficiency and facile fabrication process. Several white emission LECs based on light-emitting polymers or ionic transition metal complexes have been reported in the literature. Alkoxyphenyl or ethylene oxide-containing PF derivatives doped with lithium salts were used as active layer in LECs to obtain white light [21–23]. Poly(*p*-phenylene vinylene) derivatives containing ionic ethylene oxide or sulfonate side groups were also reported to fabricate LECs [24–26]. In those cases, additional ion-transport materials such as polyethylene oxide, trimethylolpropane ethyloxylate, and lithium salts $LiCF_3SO_3$ were added, which increased complexity of active layer and might lead to phase separation. Iridium complexes coordinating with ionic ligands were reported to achieve high-efficiency white LECs [27–32]. In this system, however, the emissive layer is comprised of two (or more) complexes to emit white light that cannot be achieved by only one individual phosphorescent material so far. Furthermore, additional ionic liquid $BMIM^+PF_6^-$ was still added despite the incorporation of ionic groups on the ligands.

In this article, we demonstrate salt-free white LECs based on PF electrolytes. A series of fluorene-benzoselenadiazole copolymers bearing different counterions, including bromo Br^-, tetrafluoroborate BF_4^-, or hexafluorophosphate PF_6^- anions were synthesized. These three anions can be interchanged by treating with appropriate ionic salts in polar solvents, which are chosen to investigate substitution effect on thermal, optical, and LEC performance of PF electrolytes. Until now, there has been no report on PF eletrolytes carrying those counterions for LEC application. Polymer main chains comprised of blue light-emitting fluorene segments and electron-deficient 2,1,3-benzoselenadiazole were designed to produce white light. Beside, ionic side chains on C-9 position of fluorene were built for carrier injection and transportation, i.e., no additional salt would be added. The thermal, optical, as well as electrochemical properties of the synthesized polymers were investigated to understand the influence of different counterions. Finally, single-component white emission LECs were fabricated and evaluated. White electroluminescent (EL) spectra with Commission Internationale de l'Eclairage (CIE) coordinates approaching (0.33, 0.33) and high color rendering index (CRI) > 85 were obtained in this study.

According to synthetic scheme 1, the polymer **P1** was synthesized from three monomers 2,7-bis(4,4,5,5-tetramethyl-1,3,2-dioxaborolan-2-yl)-9,9-bis(6-bromo hexyl) fluorene (**M1**), 9,9-bis(6-bromohexyl)-2,7-dibromofluorene (**M2**), and 4,7-dibromo-2,1,3-benzoselenadiazole (**M3**) via the Suzuki coupling polymerization. A feed ratio of 0.25% of **M3** was introduced during polymerization to adjust the emission color of **P1**. The bromo end group was then transformed to $-N(CH_3)_3Br$ using trimethylamine in methanol to form the first ionic polymer **P1-Br**. To carry out ionic exchange reaction, **P1-Br** was treated with sodium tetrafluoroborate ($NaBF_4$) or ammonium hexafluorophosphate (NH_4PF_6) to incorporate $-N(CH_3)_3BF_4$ or $-N(CH_3)_3PF_6$ groups, respectively, to form the other two ionic polymers **P1-BF_4** or **P1-PF_6**.

2. Experimental

2.1. Characterization of materials

The synthesized materials were characterized by the following techniques. ^1H NMR spectra were recorded on a Bruker Avance 600 MHz NMR spectrometer. Gel permeation chromatography (GPC) data assembled from Viscotek with a VE3850 RI detector and three columns in series were used to measure the molecular weight distribution (MWD) relative to polystyrene standards at 35 °C. Differential scanning calorimetry was performed on a Seiko DSC 6200 unit at a heating rate of 10 °C/min and a cooling rate of 10 °C/min. TGA was undertaken on a Seiko TG/DTA 7200 instrument with a heating rate of 10 °C/min. UV–vis absorption and Photoluminescence (PL) spectra were obtained with a Princeton Instruments Acton 2150 spectrophotometer. Cyclic voltammetric measurements of the material were made in acetonitrile or methanol with 0.1 M tetrabutylammonium tetrafluoroborate ($TBABF_4$) as the supporting electrolyte at a scan rate of 50 mV/s. ITO electrodes were used as both the counter and working electrodes, and silver/silver ions (Ag in 0.1 M $AgNO_3$ solution, from Bioanalytical Systems, Inc.) was used as the reference electrode. Ferrocene was used as an internal standard, and the potential values were obtained and converted to vs SCE (saturated calomel electrode). The corresponding highest-occupied molecular orbital (HOMO) and lowest-unoccupied molecular orbital (LUMO) energy levels were estimated from the onset redox potentials.

2.2. Synthesis

2.2.1. Preparation of monomers

Three monomers **M1**–**M3** were prepared according to previous literatures [33,34].

2.2.2. Synthesis of *P1*

To a mixture of **M1** (0.3234 g, 0.4975 mmol), **M2** (0.372 g, 0.5 mmol), **M3** (0.85 mg, 0.0025 mmol), and tetrakis(triphenylphosphine)palladium (0.02 g, 0.017 mmol) was added distilled toluene (10 mL) and 2 M $K_2CO_{3(aq)}$ (10 mL) using syringe under nitrogen atmosphere. The reaction mixture was heated to 90 °C and stirred for 72 h. The resulting solution was then poured into 100 mL of methanol, and crude product was collected and re-precip-

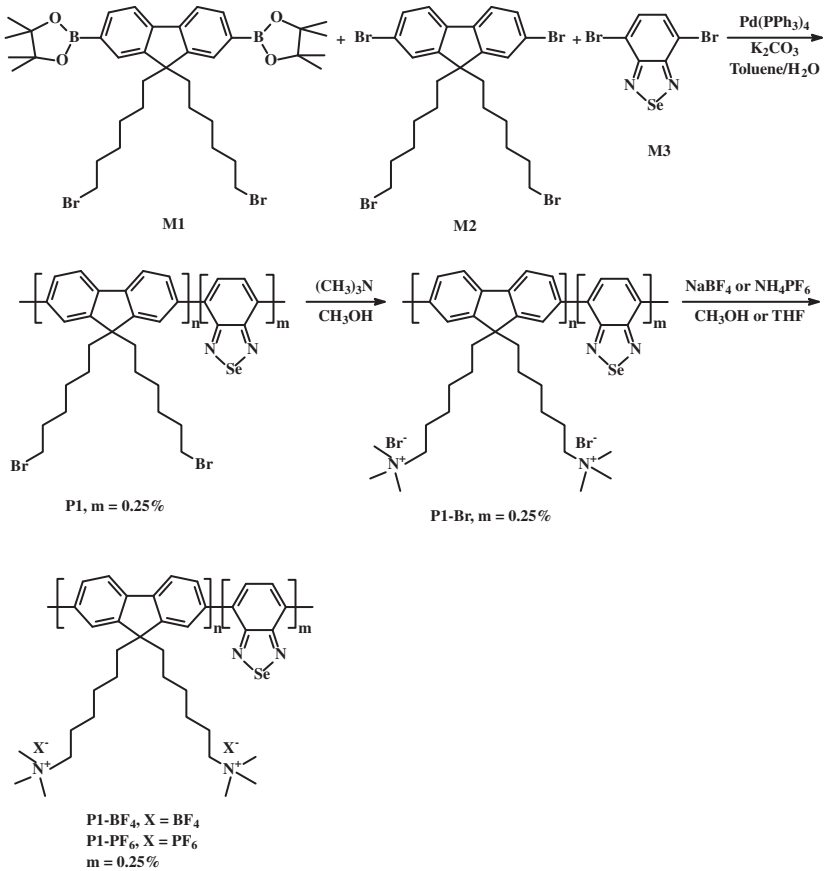

Scheme 1. Synthesis of PF electrolytes bearing different counterions.

itated in THF/methanol (2/1 in volume ratio) twice to give a yellow-greenish solid (0.35 g, 72%).

*2.2.3. Synthesis of **P1-Br***

To a solution of **P1** (100 mg) in THF (10 mL) was added 30% trimethylamine$_{(aq)}$ (5 mL) at −78 °C under nitrogen atmosphere. The mixture was stirred at room temperature for 24 h. The solvent was then removed by rotary evaporation, and crude product was re-precipitated in acetone twice to give a yellow-brown solid (92 mg, 74%).

*2.2.4. Synthesis of **P1-BF$_4$***

To a solution of **P1-Br** (100 mg) in methanol (20 mL) was slowly added a solution of $NaBF_4$ (0.528 g, 4.8 mmol) in de-ionized water (20 mL). The mixture was stirred at room temperature for 48 h, followed by removing the solvent by rotary evaporation. The previous procedure was repeated for 4 or 5 times to achieve high percentage of ionic exchange from Br to BF_4. The final product was collected and dried in oven as a yellow solid (80 mg, 78%).

2.2.5. Synthesis of P1-PF$_6$

To a solution of **P1-Br** (100 mg) in methanol (20 mL) was slowly added a solution of NH_4PF_6 (0.4 g, 4.8 mmol) in de-ionized water (20 mL). The mixture was stirred at room temperature for 48 h, followed by removing the solvent by rotary evaporation. The previous procedure was repeated for 4 or 5 times to achieve high percentage of ionic exchange from Br to PF_6. The final product was collected and dried in oven as a yellow solid (79 mg, 77%).

2.3. LEC device fabrication and characterization

ITO-coated glass substrates were cleaned and treated with UV/ozone prior to use. A PEDOT:PSS layer (30 nm) was spin-coated at 4000 rpm onto the ITO substrate in air and baked at 150 °C for 30 min. The emissive layer was then spin-coated at 3000 rpm from acetonitrile solutions. The thicknesses of thin films of **P1-BF$_4$** spin-coated from solutions with concentrations of 50 and 150 mg/mL are 180 and 370 nm, respectively. The thicknesses of thin films of **P1-PF$_6$** spin-coated from solutions with concentrations of 50 and 150 mg/mL are 170 and 380 nm, respectively. The thickness of thin film was measured by employing ellipsonetry. All solution preparing and spin-coating processes were carried out under ambient conditions. After spin coating, the thin films were then baked at 70 °C for 10 h in a nitrogen glove box (oxygen and moisture levels below 1 ppm), followed by thermal evaporation of a 100-nm Ag top contact in a vacuum chamber ($\sim 10^{-6}$ -torr). The electrical and emission characteristics of LEC devices were measured using a source-measurement unit

and a calibrated Si photodiode. All device measurements were performed under a constant bias voltage (3.0, 3.3 and 3.5 V). The EL spectra were taken with a calibrated CCD spectrograph.

3. Results and discussion

3.1. Characterization of polymers

The polymer **P1** was synthesized from three monomers **M1**–**M3** via the Suzuki coupling polymerization. 0.25% feed ratio of **M3** was carefully introduced during polymerization to adjust the emission color of **P1**. The number-average and weight-average molecular weights of P1 were determined by GPC to be 7.1×10^3 and 2.8×10^4 g/mol, respectively, with its polydispersity index of 3.9. The molecular weights of polymers **P1-Br**, **P1-BF$_4$**, and **P1-PF$_6$** were not measured by GPC because of low solubility in THF. Since the polymer backbone of these three polymers are the same before and after ionic exchange, the molecular weights of ionic polymers are assumed to be similar to their original polymer **P1**.

The electron spectroscopy for chemical analysis (ESCA) was used to examine the ionic exchange of polymers. Fig. 1 shows the ESCA spectra of ionic polymers **P1-Br**, **P1-BF$_4$**, and **P1-PF$_6$**. For **P1-Br**, a clear peak at 400 eV is found and assigned as N *1s* signal; three discrete peaks at 260, 180, and 80 eV are assigned as Br *3s*, *3p*, and *3d* signals, respectively, which means the incorporation of trimethylammonium bromide $-N(CH_3)_3Br$ group on alkyl chain ends. For **P1-BF$_4$**, three new peaks are observed at 700, 190, 20 eV, belonging to F *1s*, B *1s*, and F *2s* signals, while Br signals are vanished, referring to successful replacement of Br^- by BF_4^-. As for **P1-PF$_6$**, two additional peaks at 195 and 150 eV (assigned as P *2s* and *2p* signals) and existence of N *1s*, F *1s*, *2s* signals also prove that Br^- is replaced by PF_6^- after ionic exchange.

The solubility test also provides evidence of ionic exchange. **P1** are soluble in many organic solvents, such as toluene, tetrahydrofuran (THF), dichloromethane, and chlorobenzene (CB), while polymers **P1-Br**, **P1-BF$_4$**, and **P1-PF$_6$** are not. **P1-Br** can be dissolved in some high polar solvents, ex. methanol, dimethyl sulfoxide (DMSO), and *N*,*N*-dimethylformamide (DMF). After ionic exchange from Br^- to BF_4^- or PF_6^-, the solubility of resulting polymers **P1-BF$_4$** and **P1-PF$_6$** is significantly decreased in methanol, indicating change of nature of ionic polymers. The selection of solvents for different ionic polymers is important in this research. The optical investigation of these polymers in solution state is performed by choosing appropriate solvents. Self-standing thin films of polymers are carefully prepared by spin-coating from their solutions using different solvents.

3.2. Thermal analysis of polymers

The thermal properties of **P1** and its corresponding ionic polymers were investigated by TGA and DSC. Fig. 2 shows the TGA thermograms of all polymers by heating from 100 to 600 °C. The decomposition temperatures T_d (defined as 5% weight loss) were determined at 298, 211, 289, and 274 °C for **P1**, **P1-Br**, **P1-BF$_4$**, and **P1-PF$_6$**, respectively. It is seen that T_d of three ionic polymers is lower than that of the original polymer **P1**, which is explained by the formation of Hofmann elimination [35]. Nguyen et al. proposed that quaternary ammonium group on the side chain is cleaved and eliminated by heating over 180 °C. Besides, it is found that T_d of **P1-BF$_4$** and **P1-PF$_6$** are much higher than that of **P1-Br**, revealing that BF_4^- and PF_6^- groups possess resistance to thermal heating. It is concluded that ionic polymers bearing PF_4^- and PF_6^- groups show improved thermal stability and bring benefit in device application, since the inner temperature is usually increased under bias operation.

The glass transition temperature T_g was determined by DSC measurement. The T_g of polymer **P1** was found at 82 °C (see Supplementary data). Moreover, the T_g of other ionic polymers is close to that of **P1**, owing to the same polymer main chain that possesses similar thermal behavior.

3.3. Optical and electrochemical properties of polymers

As mentioned previously, the selection of solvents may affect the optical properties of materials. Here we choose

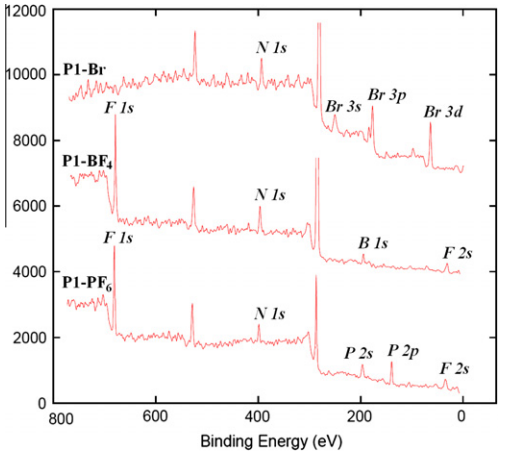

Fig. 1. ESCA spectra of polymers **P1-Br**, **P1-BF$_4$**, and **P1-PF$_6$**.

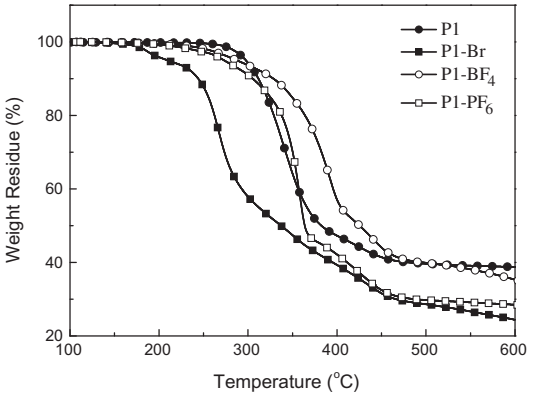

Fig. 2. TGA thermograms of polymers **P1**, **P1-Br**, **P1-BF$_4$**, and **P1-PF$_6$**.

several solvents with high dissolubility to perform the UV–vis absorption and PL emission spectroscopies. THF, toluene, and CB are used for **P1**, while polar solvents methanol, DMF, and DMSO are for **P1-Br**. As for **P1-BF_4** and **P1-PF_6**, acetonitrile, DMF, and DMSO are used to prepare their polymer solutions. The UV–vis absorption spectra of polymers in different state are depicted in Fig. 3. The absorption maxima (λ_{max}) of **P1** are located at 383 nm in solutions and 385 nm in film state (ca. 100 nm), belonging to π–π^* transition along the main chain. After ionic exchange, the λ_{max} of the forming ionic polymers **P1-Br**, **P1-BF_4**, and **P1-PF_6** are red-shifted to 384–396 nm; meanwhile, their λ_{max} in film state (ca. 100 nm) are also red-shifted to 388–400 nm. The change in absorption spectra between original and ionic polymers can be attributed to polar effect. Polymers **P1-Br**, **P1-BF_4**, and **P1-PF_6** contain many ionic groups $-N(CH_3)_3Br$, $-N(CH_3)_3BF_4$, and $-N(CH_3)_3PF_6$, leading to dissolve in those high polar solvents methanol, DMF, and DMSO, etc. The UV–vis absorprion of polymers in polar solvents usually results in red shift, as reported in the previous literature [36]. Besides, the absorption behavior of **P1** in CB, THF, and toluene are close, while other ionic polymers are distinguishable in different solvents, as shown in Fig. 3. **P1-Br** shows the bluest absorption λ_{max} at 384 nm in methanol, while **P1-BF_4** and **P1-PF_6** reveal the bluest absorption λ_{max} at 385 nm in acetonitrile. This phenomenon is explained by the highest solubility of polymers in two different solvents. It is found that **P1-Br** is highly soluble in methanol, indicating that polymer chains are surrounded and separated with each other by solvent molecules. The reduced aggregates of polymer chains results in blue shift in absorption spectrum. Same explanation can be applied to **P1-BF_4** and **P1-PF_6** with the use of acetonitrile.

The PL emission spectra of polymers in different state are shown in Fig. 4, under excitation of max. absorption wavelength. All polymers reveal only one emission band around 430 nm in solution state, resulting from the emission of PF main chain. Similar to UV–vis absorption, the emission spectra of **P1-Br** and **P1-BF_4** (as well as **P1-PF_6**) possess the bluest λ_{max} in methanol and acetonitrile, respectively. It is found that an additional yellow emission around 560 mm arises in film state, owing to the presence of electron-deficient 2,1,3-benzoselenadiazole moieties. To further investigate the formation of yellow emission, **P1**/poly(methyl methacrylate) (PMMA) composites with different concentrations of **P1** (1%, 5%, and 20%) were spin-cast into thin films from their toluene solutions. The PL properties of **P1**/PMMA composite films were then measured and shown in Fig. 5. A clear emission band around

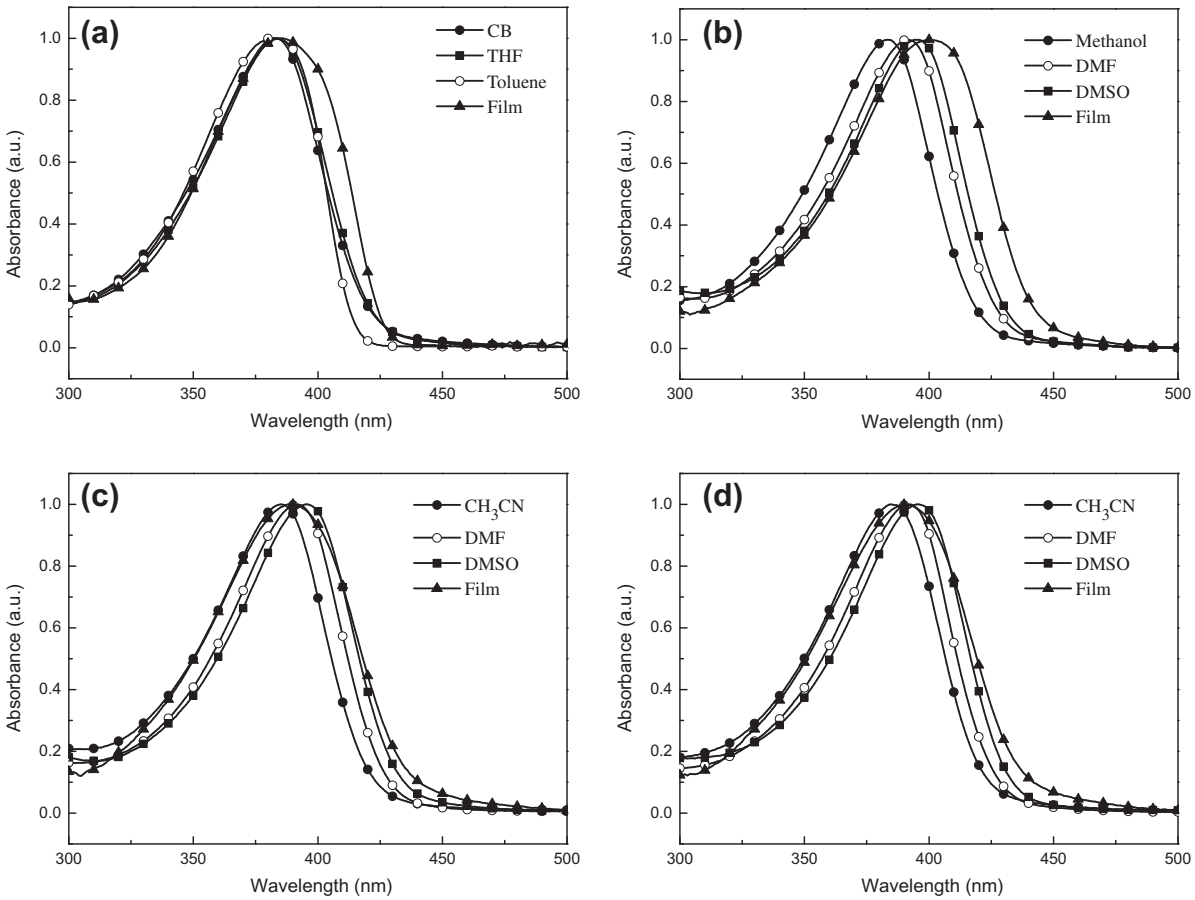

Fig. 3. UV–vis absorption spectra of polymers (a) **P1**, (b) **P1-Br**, (c) **P1-BF_4**, and (d) **P1-PF_6** in different state.

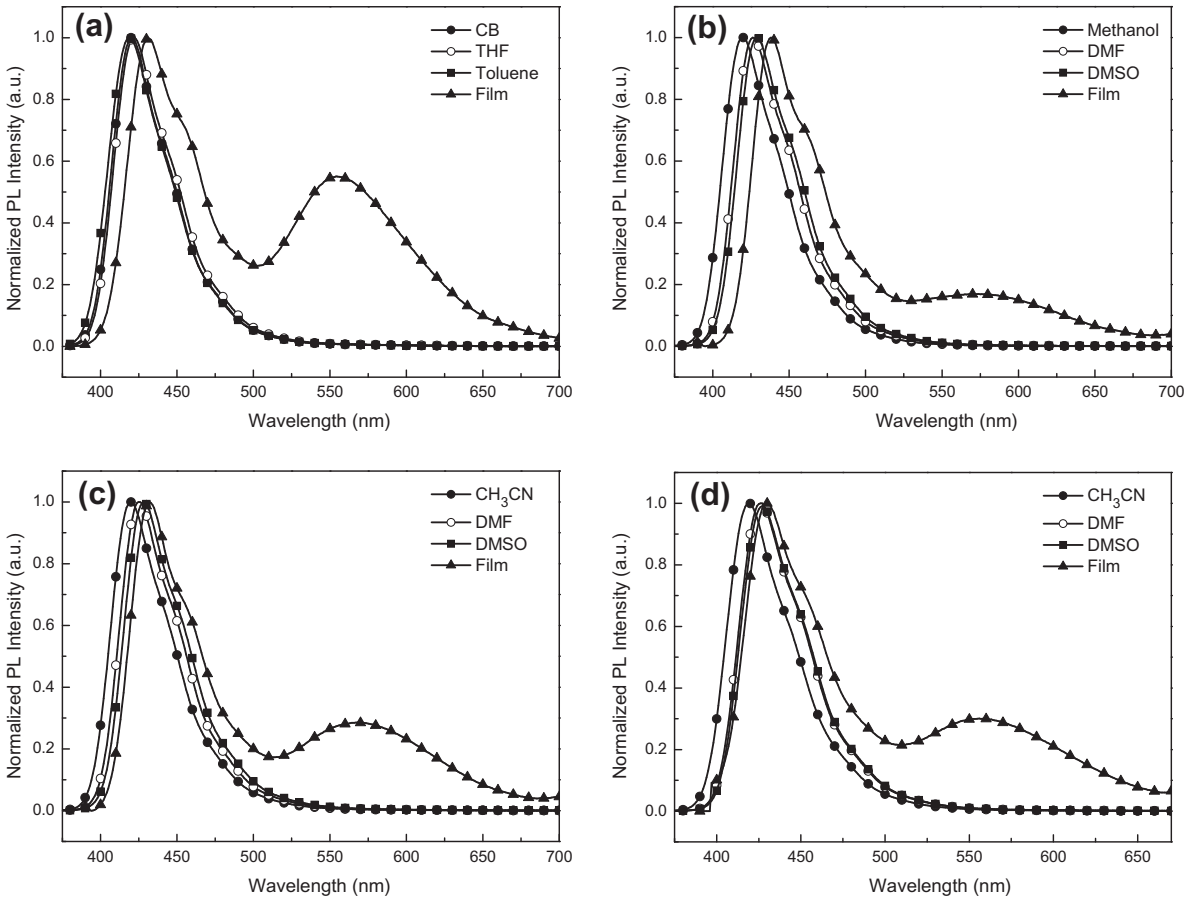

Fig. 4. PL emission spectra of polymers (a) **P1**, (b) **P1-Br**, (c) **P1-BF_4**, and (d) **P1-PF_6** in different state.

560 nm is also observed for all **P1**/PMMA composites, even for the one with very low concentration of **P1** (1%). The intensity of the yellow emission is gradually augmented as the concentration of **P1** is increased. The change in PL intensity is due to shortening intermolecular distance of **P1** in PMMA matrix and is concentration-dependent, providing an evidence of energy transfer occurred in solid state. Moreover, individual films of homopolyfluorene without 2,1,3-benzoselenadiazole moiety (denoted as **P0**) and 0.25% 2,1,3-benzoselenadiazole/PMMA composite were also prepared for comparison. It is found that **P0** film possesses only blue emission around 430 nm, while 2,1,3-benzoselenadiazole/PMMA shows no luminescent property in the visible region (see Supplementary data). It is clear that yellow emission band is resulted from the presence of 2,1,3-benzoselenadiazole along PF main chain, not related to aggregates of fluorine segments. The above results demonstrate that yellow emission band arises from energy transfer from the PF to 2,1,3-benzoselenadiazole moieties.

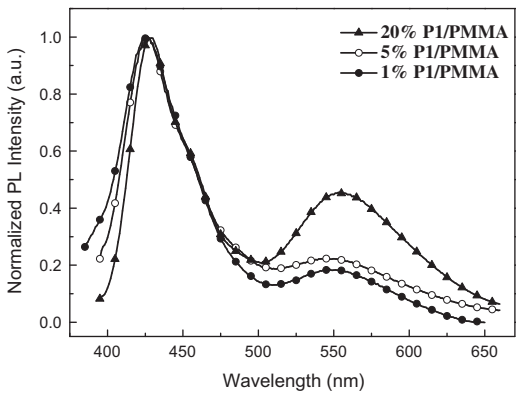

Fig. 5. PL emission spectra of **P1**/PMMA composite films with different concentration of **P1**.

One may regard a full amount of energy transfer between two moieties because of very short distance in film state; however, only partial energy transfer from the PF to 2,1,3-benzoselenadiazole is observed in our case, resulting in simultaneous emission at different wavelengths. This can be attributed to very low feed ratio of the heterocyclic monomer **M3** (0.25% in molar ratio). It is reported that only 1% of the fluorenone defects can almost completely quench blue fluorescence of the PF [37]. Cao et al. demonstrated effective energy transfer from the PF to heterocyclic rings with a small amount of benzothiadiazole or benzoselen-

adiazole (1–2% in molar ratio) [38,39]. In this study we further reduced added amount of monomer **M3** during polymerization, and simultaneous emission was obtained successfully. Besides, larger twist angle between neighboring rings (fluorine and benzoselenadiazole) may also hinder energy transfer. Combining two bands around 430 and 560 nm would bring white emission that can be utilized for lighting application. Other methods, such as binary blends of a blue light-emitting polymer and an encapsulated green/yellow emissive polymer with functionalized cyclodextrins, have also been reported to achieve white emission, and the amount of the encapsulated material can be increased up to 20% by weight [40].

Furthermore, it is observed that intensity of the yellow emission band is decreased as quaternary ammonium group is tethered, as seen in Fig. 4b–d. The reason to this phenomenon is explained as follows. Firstly, it is noted that the difference between **P1** and ionic polymers (**P1-Br**, **P1-BF_4**, **P1-PF_6**) is the attachment of ionic groups. Secondly, the heterocyclic 2,1,3-benzoselenadiazole is known as an electron-deficient moiety; the nature of quaternary ammonium groups $-N(CH_3)_3Br$, $-N(CH_3)_3BF_4$, and $-N(CH_3)_3PF_6$ are also electron-transport dominating. Both 2,1,3-benzoselenadiazole and ion groups can act as electron trapper. As electrons are attracted to stay on those ionic side groups instead of 2,1,3-benzoselenadiazole moieties, the energy transfer from the PF to 2,1,3-benzoselenadiazole would be reduced. The competition between these two moieties would lower the probability of exciton association on 2,1,3-benzoselenadiazole and, in consequence, decrease yellow emission band for those ionic polymers.

To further understand the optical property of these polymers, absolute PL quantum yield (PLQY) is recorded using integrating sphere with an excitation wavelength of 360 nm. The values of PLQY for **P1**, **P1-Br**, **P1-BF_4**, and **P1-PF_6** are measured to be 58%, 80%, 72%, 85% in solution, and 13%, 10%, 13%, 16% in film state. It is seen that ionic polymers **P1-Br**, **P1-BF_4**, and **P1-PF_6** show higher PLQY values compared with their original polymer **P1**, implying loose and expanded chain packing in solution due to the strong repulsion between charged side groups [36]. On the other hand, PLQYs of all polymers are significantly decreased in film compared with those in solution, due to energy loss between close packed chains in solid state. For neutral polymers the loss in PLQY (as well as energy) is mainly due to formation of aggregates with reduced oscillator strengths from their solution to solid state. After quaternization, the PLQY of ionic polymers could be further reduced compared with their neutral precursors. This phenomenon is interpreted by the presence of ions that can act as luminescent quenchers by favoring exciton dissociation via coulombic interactions of the charges with the excitonic species. Very low PLQY of 4.7–8.3% has been reported for PF and benzene-fluorene copolymer electrolytes tethering $-N(CH_3)_3Br$ groups [36]. In our case **P1-Br** showed a lower PLQY compared with **P1**, while **P1-BF_4** and **P1-PF_6** own similar values in solid state. To increase PLQY as well as EL efficiencies, one can utilize encapsulation architecture to prevent interactions between polymer chains. There have been several reports on cyclodextrin-encapsulated conjugated polymers that show an increase in PLQY by a factor of 2.5–5 compared with un-thread ones; for some cases the PLQY even maintains at the same level both in solution and solid states [41–43].

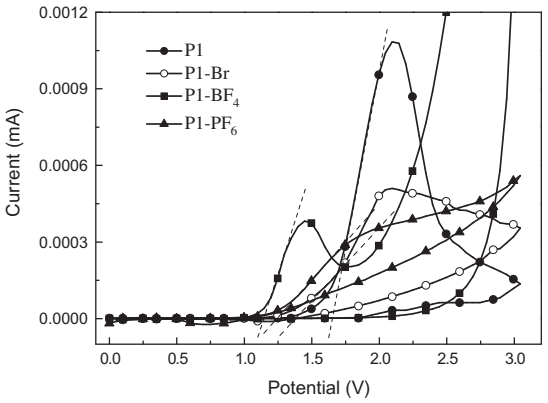

Fig. 6. Cyclic voltammograms of polymers **P1**, **P1-Br**, **P1-BF_4**, and **P1-PF_6** in the oxidation process.

Cyclic voltammetry (CV) was employed to investigate the electrochemical behaviors of synthesized polymers and to estimate their energy levels. To our best knowledge, the energy levels of ionic polymers have not been reported in the previous literature. Fig. 6 shows cyclic voltammograms of all polymers in the oxidation process. One can observe that the onset of oxidation potential for three ionic polymers **P1-Br**, **P1-BF_4**, and **P1-PF_6** is decreased, which is favored for hole injection. The highest-occupied molecular orbital (HOMO) levels of **P1**, **P1-Br**, **P1-BF_4**, and **P1-PF_6** are then determined to be −6.03, −5.87, −5.53, and −5.64 eV, respectively. Furthermore, energy gaps (EG) of polymers are estimated according to previous literature in the range of 2.85 and 2.91 eV [44]. The lowest-unoccupied molecular orbital (LUMO) levels are thus calculated to be −3.12, −2.99, −2.66, and −2.78 eV for polymers **P1**, **P1-Br**, **P1-BF_4**, and **P1-PF_6**, respectively. From CV measurement it is concluded that the attachment of quaternary ammonium groups results in increased energy levels.

3.4. Fabrication and evaluation of LEC devices

EL characteristics of white LECs based on **P1-BF_4** and **P1-PF_6** were measured and summarized in Table 1. It is noted that devices based on **P1-Br** are not involved since they are rather unstable under electrical driving. It would be attributed to the degradation of polymers caused by Hofmann elimination, as discussed in the Section 3.2. The white LECs have the structure of indium tin oxide (ITO) (120 nm)/poly(3,4-ethylenedioxythiophene):poly(styrene sulfonate) (PEDOT:PSS) (30 nm)/emissive layer/Ag (100 nm), where the emissive layer is a thin film of **P1-BF_4** (180 nm), **P1-BF_4** (370 nm), **P1-PF_6** (170 nm), and **P1-PF_6** (380 nm) for each device. The EL spectra of white LECs based on **P1-BF_4** under various bias voltages (the same thickness of the emissive layer, 275 nm) and in various thicknesses of the emissive layers (the same bias voltage, 3 V) are shown in Fig. 7a and b, respectively. Simultaneous EL emissions from the blue emitting fluorene

Table 1
Summary of EL characteristics of white LECs.

Device	Bias (V)	t_{max} (s)[a]	J_{max} (mA cm^{-2})[b]	L_{max} (cd m^{-2})[c]	$\eta_{ext,max}$ (%)[d]	$\eta_{p,max}$ (lm W^{-1})[e]	Lifetime (s)[f]	CIE (x,y)[g]	CRI[h]
P1-BF$_4$ (180 nm)	3.0	30	11	54	0.29	0.55	550	(0.321, 0.323)	86
	3.3	30	69	297	0.24	0.42	170	(0.254, 0.244)	94
	3.5	20	116	440	0.24	0.34	140	(0.234, 0.207)	–[i]
P1-BF$_4$ (370 nm)	3.0	540	2	17	0.40	0.79	1540	(0.241, 0.327)	60
	3.3	130	53	151	0.30	0.43	700	(0.332, 0.429)	65
	3.5	60	120	226	0.17	0.31	320	(0.220, 0.279)	65
P1-PF$_6$ (170 nm)	3.0	550	28	4	0.04	0.09	910	(0.273, 0.251)	86
	3.3	160	52	30	0.09	0.14	250	(0.247, 0.230)	81
	3.5	140	56	43	0.11	0.15	110	(0.245, 0.213)	–[i]
P1-PF$_6$ (380 nm)	3.0	990	1	13	0.69	1.56	2130	(0.360, 0.383)	72
	3.3	500	10	113	0.66	1.28	790	(0.299, 0.343)	72
	3.5	320	30	231	0.55	0.95	440	(0.309, 0.344)	71

[a] Time required to reach the maximal brightness.
[b] Maximal current density achieved at a constant bias voltage.
[c] Maximal brightness achieved at a constant bias voltage.
[d] Maximal external quantum efficiency achieved at a constant bias voltage.
[e] Maximal power efficiency achieved at a constant bias voltage.
[f] The time for the brightness of the device to decay from the maximum to half of the maximum under a constant bias voltage.
[g] CIE coordinates calculated from the EL spectra.
[h] Color rendering index calculated from the EL spectra.
[i] Undefined CRI for this spectrum.

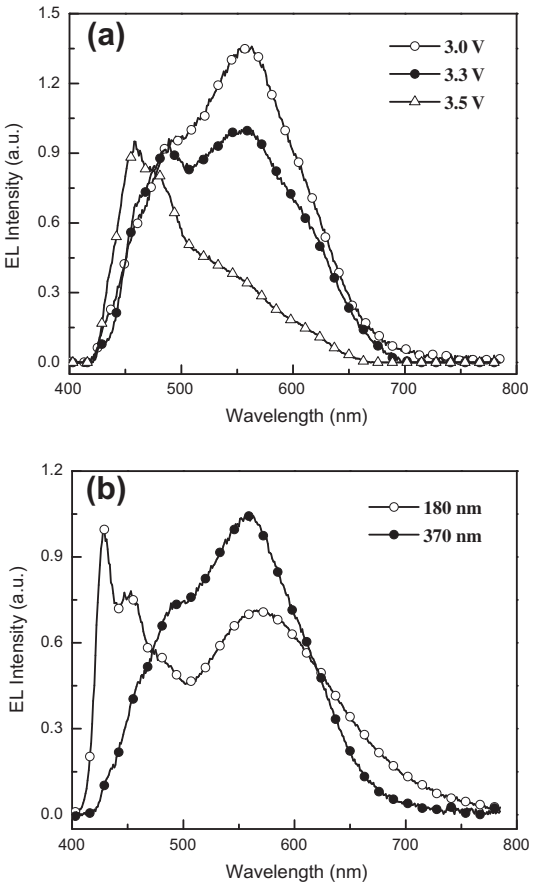

Fig. 7. Comparison of the EL spectra of white LECs based on **P1-BF$_4$** (a) under various bias voltages (the same thickness of the emissive layer, 370 nm) and (b) in various thicknesses of the emissive layers (the same bias voltage, 3 V).

segments and the yellow emitting 2,1,3-benzoselenadiazole moieties were measured in all devices based on **P1-BF$_4$**. However, the bias voltage and the thickness of the emissive layer affect the relative amount of the yellow emission with respect to the blue one, resulting in altered white EL spectra. In these white LECs, electrochemically doped regions of the emissive layer result in ohmic contact with metal electrodes and consequently facilitate carrier injection onto both the fluorene segments and the 2,1,3-benzoselenadiazole moieties. Hence, both exciton formation on the higher-gap fluorene followed by energy transfer to the lower-gap 2,1,3-benzoselenadiazole and direct exciton formation on the lower-gap 2,1,3-benzoselenadiazole induced by charge trapping contribute to the yellow emission. At a lower bias, e.g., 3 V, carrier injection and trapping on the smaller-gap 2,1,3-benzoselenadiazole would be favored and thus direct exciton formation on the lower-gap chromophore would lead to more significant yellow emission (Fig. 7a, 3.0 V). As the bias increases, carrier injection and exciton formation on the higher-gap fluorene is facilitated and subsequent partial energy transfer dominates the yellow emission, resulting in less significant yellow emission (Fig. 7a, 3.3 and 3.5 V). The thickness of the emissive layer also affects the EL spectra. When biased under the same voltage, a lower electric field in a thicker device would impede carrier injection onto the higher-gap fluorene. Hence, direct exciton formation on the lower-gap chromophore is preferred and more significant yellow emission in a thicker device is observed (Fig. 7b, 275 nm). On the contrary, a higher electric field in a thinner device facilitates carrier injection onto the higher-gap fluorene. Yellow emission mainly comes from partial energy transfer from blue excitons on the fluorene and thus reduced yellow emission is present in the EL spectrum (Fig. 7b, 180 nm). EL spectra of **P1-PF$_6$** exhibited similar evolution trends when the bias voltage and the thickness

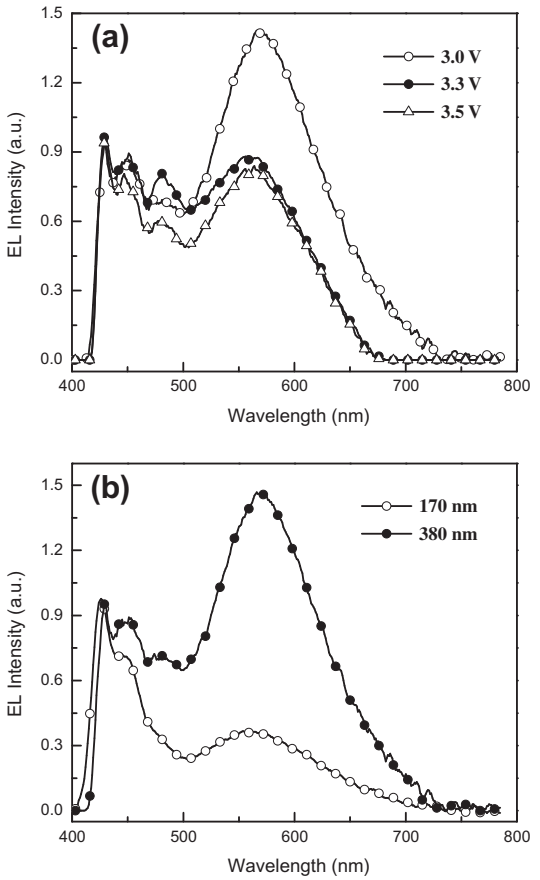

Fig. 8. Comparison of the EL spectra of white LECs based on **P1-PF$_6$** (a) under various bias voltages (the same thickness of the emissive layer, 380 nm) and (b) in various thicknesses of the emissive layers (the same bias voltage, 3 V).

of the emissive layer are varied (Fig. 8a and b). These results show that white LECs based on these PF electrolytes show CIE coordinates close to (0.33, 0.33) and good CRI > 85, which are essential for solid-state lighting applications.

All white LECs based on copolymers **P1-BF$_4$** and **P1-PF$_6$** showed similar time-dependent EL characteristics. The time-dependent brightness and current density of Device **P1-BF$_4$** (370 nm) under constant biases of 3.0–3.5 V are shown in Fig. 9a. After the bias was applied, the device current first rose and then stayed rather constant. On the other hand, the brightness first increased with the device current, reaching maximum values before undergoing gradual decreases over time. The time required for the brightness to reach its maximum value decreased as the bias voltage increased (Table 1), presumably because a higher accumulation rate of mobile ions facilitated the formation of electrochemically doped regions under a higher electric field. The maximum brightness of Device **P1-BF$_4$** (370 nm) reached 17, 151, and 226 cd/m^2 under biases of 3.0, 3.3 and 3.5 V, respectively. The brightness then dropped with time with a rate depending on the bias voltage (or current). Under a constant bias, the lifetime of each device, defined as the time required for the brightness of

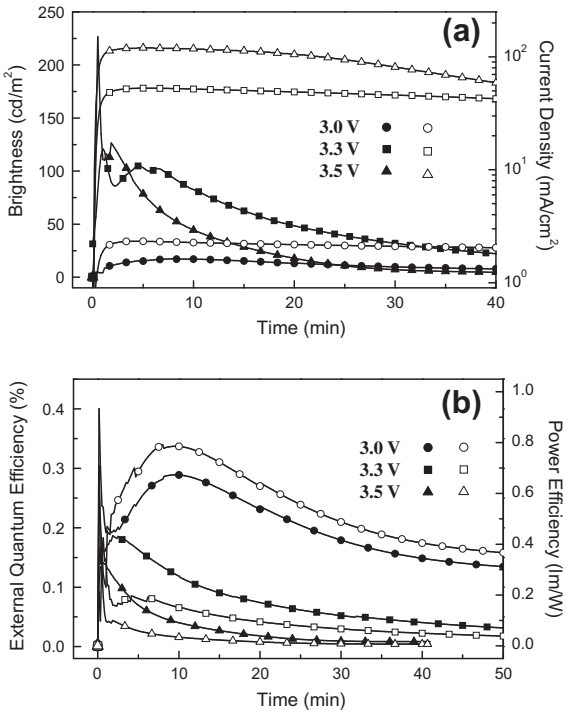

Fig. 9. (a) Brightness (solid symbols) and current density (open symbols) and (b) external quantum efficiency (solid symbols) and power efficiency (open symbols) as a function of time under a constant bias voltage of 3.0–3.5 V for Device **P1-BF$_4$** (370 nm).

the device to decay from the maximum value to half of the maximum value, decreased upon increasing the bias voltage (Table 1). It results from that higher current density induced by a higher bias voltage led to a higher rate of irreversible multiple oxidation and subsequent decomposition of the emissive material, thereby accelerating the degradation of the LEC devices [45]. The external quantum efficiency (EQE) and power efficiency of Device **P1-BF$_4$** (370 nm) under constant biases of 3.0–3.5 V are shown in Fig. 9b. Immediately after a forward bias was applied, the EQE was rather low because of unbalanced carrier injection. During the formation of the doped regions near the electrodes, the balance of the carrier injection was improved and, accordingly, the EQE of the device increased rapidly. The peak EQE and peak power efficiency for Device **P1-BF$_4$** (370 nm) under 3 V were 0.4% and 0.79 lm W^{-1}, respectively. The drop of efficiencies after reaching the peak value, as commonly seen in solid-state LECs [46–51], may be attributed to a few factors. Before the device current reaches a steady value, the thickness of the intrinsic layer between the *p*- and *n*-type doped layers is gradually reduced and thus the electric field in the intrinsic layer increases with time [52]. The recombination zone in the intrinsic layer may keep moving closer to one electrode due to discrepancy in electron and hole mobilities under a varying electric field, which would induce exciton quenching. After reaching a steady device current, the decrease in efficiencies under a constant bias was irreversible and thus may be rationally associated with the degradation of the emissive material during the LEC operation [53]. The

thickness of the emissive layer also affects the time-dependent EL characteristics. In a thinner device **P1-BF$_4$** (180 nm), a higher electric field accelerates accumulation of mobile ions and fastens device response in consequence (Table 1). Furthermore, a higher electric field also results in a higher device current and thus a higher brightness (Table 1). A thicker emissive layer is beneficial in keeping the recombination zone away from the doped regions. Hence, exciton quenching near the doped regions [54], in which the ion density would be high, would be mitigated and device efficiencies would thus be enhanced. In addition, a lower electric field in a thicker emissive layer reduces device current and thus leads to improved device stability (Table 1, cf. Device **P1-BF$_4$** (180 nm) and **P1-BF$_4$** (370 nm)). The time-dependent brightness/current density and EQE/power efficiency of Device **P1-PF$_6$** (380 nm) under constant biases of 3.0–3.5 V are shown in Fig. 10a and b, respectively. Replacing the BF_4^- anions with larger PF_6^- anions did not significantly alter the trend in the time-dependent EL characteristics of the white LECs. However, the device response is slower in devices containing larger PF_6^- anions due to a lower ionic mobility of larger anions in the emissive layer (Table 1) [55]. In addition, devices employing PF_6^- counterions exhibited lower device current density and thus longer device lifetimes were obtained (Table 1). It is noted that the thicker device using PF_6^- counterions (Device **P1-PF$_6$** (380 nm)) showed high peak EQE and power efficiency up to 0.69% and 1.56 lm W^{-1}, respectively. These results are approaching the upper limit (~0.8%) that one would expect from the PLQY of the thin film of **P1-PF$_6$** (16%, see Section 3.3) when fluorescent spin statistics of ca. 25% and an optical out-coupling efficiency of ca. 20% are estimated. Thus, superior carrier balance in white LECs based on **P1-PF$_6$** could be speculated. It may result from the bipolar characteristic of the molecular structure of **P1-PF$_6$**, which is consisted of hole transporting fluorene segments and electron transporting 2,1,3-benzoselenadiazole moieties. Such device efficiencies are among the highest reported for white-light polymer LECs [15,16]. Furthermore, white EL spectra with CIE coordi-

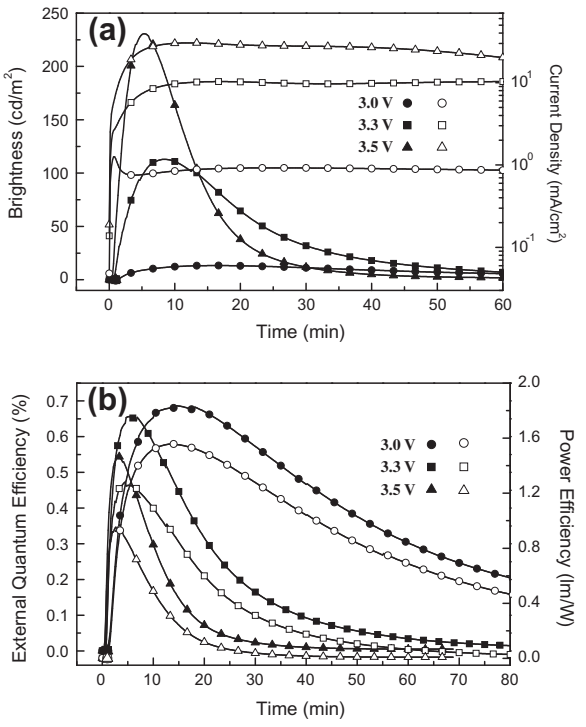

Fig. 10. (a) Brightness (solid symbols) and current density (open symbols) and (b) external quantum efficiency (solid symbols) and power efficiency (open symbols) as a function of time under a constant bias voltage of 3.0-3.5 V for Device **P1-PF$_6$** (380 nm).

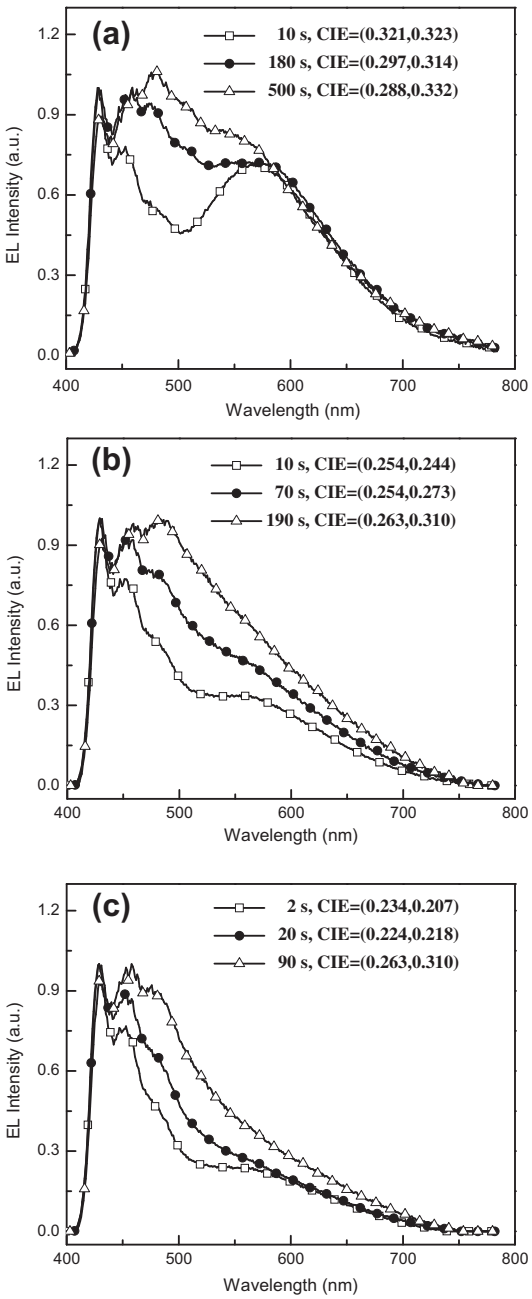

Fig. 11. Time-dependent EL spectra for Device **P1-BF$_4$** (180 nm) under (a) 3.0, (b) 3.3 and (c) 3.5 V. Corresponding CIE coordinates of the EL spectra are shown in the inset.

nates approaching (0.33, 0.33) and high CRIs > 85 have been reported for the first time in polymer white LECs to the best of our knowledge.

To examine the color stability of the white LECs, time-dependent EL spectra of devices based on **P1-BF$_4$** and **P1-PF$_6$** were measured and are shown in Figs. 11 and 12, respectively. Both white LECs based on **P1-BF$_4$** and **P1-PF$_6$** exhibited enhanced green emission and thus resulted in color shift over time. Such green emission was also observed in fluorene-based LECs [21], and would be attributed to the electrooxidized cleavage of C9-substituted alkyl pendant groups [55]. The color migrations in the CIE coordinates (Δx, Δy) are (0.033, 0.018), (0.009, 0.066) and (0.039, 0.103) for Device **P1-BF$_4$** (180 nm) under 3.0, 3.3 and 3.5 V, respectively. For Device **P1-PF$_6$** (170 nm), (Δx, Δy) are (0.037, 0.067), (0.021, 0.016) and (0.026, 0.015) under 3.0, 3.3 and 3.5 V, respectively. These results are comparable with that of reported host–guest white polymer LECs ((Δx, Δy) = (0.08, 0.03)) [23], in which the color migration comes from carrier trapping of the low-gap guest. However, even when electrooxidation of the fluorene moiety occurred, the color stability of the single-component white LECs is not worse than that of the host-guest white LECs. With similar color stability, single-component white LECs are promising since additionally they are free from phase separation and can be fabricated more easily and reproducibly as compared to multi-component host-guest white LECs. Further improvement in color stability of single-component white LECs could be expected when peripheral aryl substituents are tethered on the C9 position and related studies are underway [23].

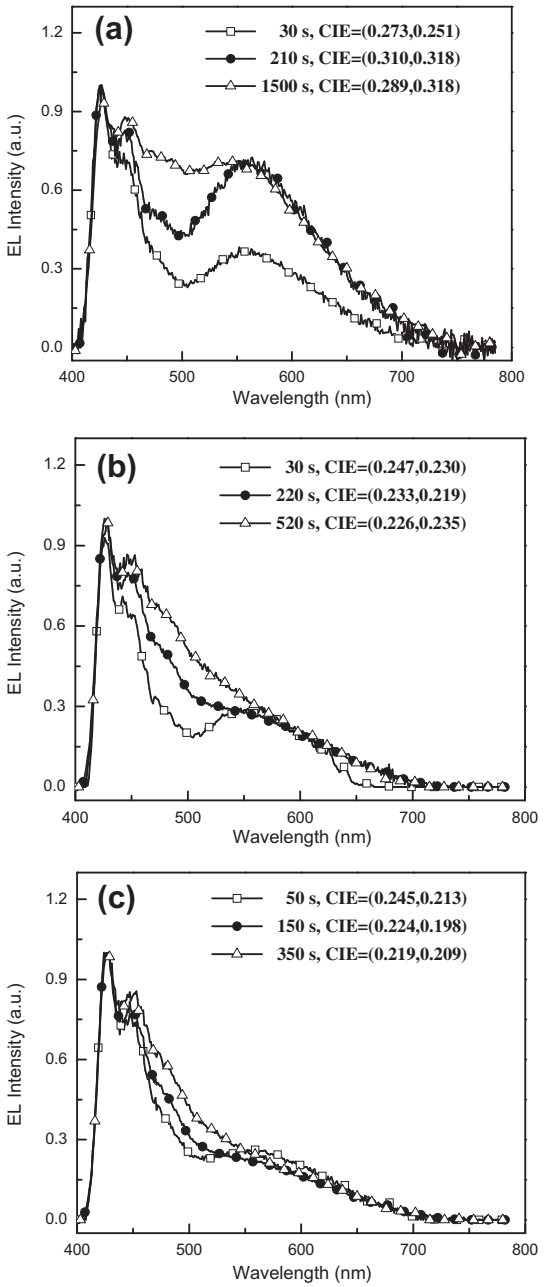

Fig. 12. Time-dependent EL spectra for Device **P1-PF$_6$** (170 nm) under (a) 3.0, (b) 3.3 and (c) 3.5 V. Corresponding CIE coordinates of the EL spectra are shown in the inset.

4. Conclusion

A series of PF electrolytes bearing Br^-, BF_4^-, and PF_6^- counterions on the side chains were synthesized and characterized. Electron-deficient 2,1,3-benzoselenadiazole moieties were copolymerized into PF main chains to produce white light. Polymers **P1-BF$_4$** and **P1-PF$_6$** were found to suppress the formation of Hoffmann elimination and to increase thermal stabilities. All polymers showed two emission bands around 430 and 560 nm in thin film state; in addition, the intensity of the yellow emission band was decreased as quaternary ammonium group is tethered. Electrochemical analysis revealed that oxidation potentials of **P1-BF$_4$** and **P1-PF$_6$** were significantly decreased compared to their original polymer P1. Single-component white LECs were fabricated using **P1-BF$_4$** and **P1-PF$_6$** as active layer, without adding additional inorganic salts. Characteristics including high luminescence efficiency of 1.56 lm/W, pure white EL emission, and high CRI values demonstrated the best device result among white-light polymer LECs so far.

Acknowledgement

The authors thank the National Science Council of the Republic of China (NSC 100-2113-M-009-012-MY2) for financial support of this work.

Appendix A. Supplementary material

Supplementary data associated with this article can be found, in the online version, at http://dx.doi.org/10.1016/j.orgel.2012.11.029.

References

[1] A.C. Grimsdale, K.L. Chan, R.E. Martin, P.G. Jokisz, A.B. Holmes, Chem. Rev. 109 (2009) 897.

[2] Y.J. Cheng, S.H. Yang, C.S. Hsu, Chem. Rev. 109 (2009) 5868.
[3] D.S. Chung, S.J. Lee, J.W. Park, D.B. Choi, D.H. Lee, J.W. Park, S.C. Shin, Y.H. Kim, S.K. Kwon, C.E. Park, Chem. Mater. 20 (2008) 3450.
[4] X. Chen, J.L. Liao, Y. Liang, M.O. Ahmed, H.E. Tseng, S.A. Chen, J. Am. Chem. Soc. 125 (2002) 636.
[5] P. Herguth, X. Jiang, M.S. Liu, A.K.-Y. Jen, Macromolecules 35 (2002) 6094.
[6] J. Luo, X. Li, Q. Hou, J. Peng, W. Yang, Y. Cao, Adv. Mater. 19 (2007) 1113.
[7] R. Yang, A. Garcia, D. Korystov, A. Mikhailovsky, G.C. Bazan, T.Q. Nguyen, J. Am. Chem. Soc. 128 (2006) 16532.
[8] S.H. Oh, S.I. Na, Y.C. Nah, D. Vak, S.S. Kim, D.Y. Kim, Org. Electron. 8 (2007) 773.
[9] C.V. Hoven, A. Garcia, G.C. Bazan, T.Q. Nguyen, Adv. Mater. 20 (2008) 3793.
[10] J. Fang, B.H. Wallikewitz, F. Gao, G. Tu, C. Müller, G. Pace, R.H. Friend, W.T.S. Huck, J. Am. Chem. Soc. 133 (2011) 683.
[11] Q. Pei, G. Yu, C. Zhang, Y. Yang, A.J. Heeger, Science 269 (1995) 1086.
[12] I.V. Kosilkin, M.S. Martens, M.P. Murphy, J.M. Leger, Chem. Mater. 22 (2010) 4838.
[13] Q.B. Pei, Y. Yang, G. Yu, C. Zhang, A.J. Heeger, J. Am. Chem. Soc. 118 (1996) 3922.
[14] J.C. deMello, N. Tessler, S.C. Graham, R.H. Friend, Phys. Rev. B 57 (1998) 12951.
[15] J.C. deMello, Phys. Rev. B 66 (2002) 235210.
[16] A.J. Norell Bader, A.A. Ilkevich, I.V. Kosilkin, J.M. Leger, Nano Lett. 11 (2011) 461.
[17] J.D. Slinker, J.A. DeFranco, M.J. Jaquith, W.R. Silveira, Y. Zhong, J.M. Moran-Mirabal, H.G. Graighead, H.D. Abruña, J.A. Marohn, G.G. Malliaras, Nat. Mater. 6 (2007) 894.
[18] P. Matyba, K. Maturova, M. Kemerink, N.D. Robinson, L. Edman, Nat. Mater. 8 (2009) 672.
[19] D.B. Rodovsky, O.G. Reid, L.S.C. Pingree, D.S. Ginger, ACS Nano 4 (2010) 2673.
[20] S. Reenen van, P. Matyba, A. Dzwilewski, R.A.J. Janssen, L. Edman, M. Kemerink, J. Am. Chem. Soc. 132 (2010) 13776.
[21] Y. Yang, Q. Pei, J. Appl. Phys. 81 (1997) 3294.
[22] M. Sun, C. Zhong, F. Li, Y. Cao, Q. Pei, Macromolecules 43 (2010) 1714.
[23] S. Tang, J. Pan, H. Buchholz, L. Edman, Appl. Mater. Interfaces 3 (2011) 3384.
[24] J. Morgado, R.H. Friend, F. Cacialli, B.S. Chuah, S.C. Moratti, A.B. Holmes, J. Appl. Phys. 86 (1999) 6392.
[25] Z. Gu, Q.D. Shen, J. Zhang, C.Z. Yang, Y.J. Bao, J. Appl. Polym. Sci. 100 (2006) 2930.
[26] Z. Gu, Y.J. Bao, Y. Zhang, M. Wang, Q.D. Shen, Macromolecules 39 (2006) 3125.
[27] H.C. Su, H.F. Chen, F.C. Fang, C.C. Liu, C.C. Wu, K.T. Wong, Y.H. Liu, S.M. Peng, J. Am. Chem. Soc. 130 (2008) 3413.
[28] L. He, J. Qiao, L. Duan, G. Dong, D. Zhang, L. Wang, Y. Qiu, Adv. Funct. Mater. 19 (2009) 2950.
[29] L. He, L. Duan, J. Qiao, G. Dong, L. Wang, Y. Qiu, Chem. Mater. 22 (2010) 3535.
[30] H.C. Su, H.F. Chen, Y.C. Shen, C.T. Liao, K.T. Wong, J. Mater. Chem. 21 (2011) 9653.
[31] H.B. Wu, H.F. Chen, C.T. Liao, H.C. Su, K.T. Wong, Org. Electron. 13 (2012) 483.
[32] H.C. Su, H.F. Chen, P.H. Chen, S.W. Lin, C.T. Liao, K.T. Wong, J. Mater. Chem. 22 (2012) 22998.
[33] B. Liu, G.C. Bazan, J. Am. Chem. Soc. 128 (2006) 1188.
[34] X. Guo, C. Qin, Y. Cheng, Z. Xie, Y. Geng, X. Jing, F. Wang, L. Wang, Adv. Mater. 21 (2009) 3682.
[35] C.Y. Lin, A. Garcia, P. Zalar, J.Z. Brzezinski, T.Q. Nguyen, J. Phys. Chem. C 114 (2010) 15786.
[36] F. Huang, H. Wu, D. Wang, W. Yang, Y. Cao, Chem. Mater. 16 (2004) 708.
[37] P. Scandiucci de Freitas, U. Scherf, M. Collon, E.J.W. List, e-Polymers No. 009, 2002.
[38] F. Huang, L. Hou, H. Wu, X. Wang, H. Shen, W. Cao, W. Yang, Y. Cao, J. Am. Chem. Soc. 126 (2004) 9845.
[39] R. Yang, R. Tian, Q. Hou, W. Yang, Y. Cao, Macromolecules 36 (2003) 7453.
[40] S. Brovelli, G. Sforazzini, M. Serri, G. Winroth, K. Suzuki, F. Meinardi, H.L. Anderson, F. Cacialli, Adv. Funct. Mater. 22 (2012) 4284.
[41] J.S. Wilson, M.J. Frampton, J.J. Michels, L. Sardone, G. Marletta, R.H. Friend, P. Samorì, H.L. Anderson, F. Cacialli, Adv. Mater. 17 (2005) 2659.
[42] S. Brovelli, G. Latini, M.J. Frampton, S.O. McDonnell, F.E. Oddy, O. Fenwick, H.L. Anderson, F. Cacialli, Nano Lett. 8 (2008) 4546.
[43] S. Brovelli, F. Meinardi, G. Winroth, O. Fenwick, G. Sforazzini, M.J. Frampton, L. Zalewski, J.A. Levitt, F. Marinello, P. Schiavuta, K. Suhling, H.L. Anderson, F. Cacialli, Adv. Funct. Mater. 20 (2010) 272.
[44] K.B. Chen, H.C. Li, C.K. Chen, S.H. Yang, B.R. Hsieh, C.S. Hsu, Macromolecules 38 (2005) 8617.
[45] S.T. Parker, J.D. Slinker, M.S. Lowry, M.P. Cox, S. Bernhard, G.G. Malliaras, Chem. Mater. 17 (2005) 3187.
[46] Y. Shao, G.C. Bazan, A.J. Heeger, Adv. Mater. 19 (2007) 365.
[47] J.D. Slinker, J. Rivnay, J.S. Moscowitz, J.B. Parker, S. Bernhard, H.D. Abruña, G.G. Malliaras, J. Mater. Chem. 17 (2007) 2976.
[48] Y. Shao, X. Gong, A.J. Heeger, M. Liu, A.K.-Y. Jen, Adv. Mater. 21 (2009) 1972.
[49] J. Fang, P. Matyba, L. Edman, Adv. Funct. Mater. 19 (2009) 2671.
[50] T. Hu, L. He, L. Duan, Y. Qiu, J. Mater. Chem. 22 (2012) 4206.
[51] R.D. Costa, E. Ortí, H.J. Bolink, F. Monti, G. Accorsi, N. Armaroli, Angew. Chem. Int. Ed. 51 (2012) 8178.
[52] M. Lenes, G. Garcia-Belmonte, D. Tordera, A. Pertegás, J. Bisquert, H.J. Bolink, Adv. Funct. Mater. 21 (2011) 1581.
[53] G. Kalyuzhny, M. Buda, J. McNeill, P. Barbara, A.J. Bard, J. Am. Chem. Soc. 125 (2003) 6272.
[54] D.J. Dick, A.J. Heeger, Y. Yang, Q. Pei, Adv. Mater. 8 (1996) 985.
[55] H. Rudmann, S. Shimada, M.F. Rubner, J. Am. Chem. Soc. 124 (2002) 4918.